

DFTT 69/94

DTP/95/02

December 1994

**Heavy Higgs production and decay via  
 $e^+e^- \rightarrow Z^0 H^0 \rightarrow b\bar{b}Z^0 Z^0$  and irreducible backgrounds  
 at Next Linear Colliders.<sup>1</sup>**

Stefano Moretti

*Dipartimento di Fisica Teorica, Università di Torino,  
 and I.N.F.N., Sezione di Torino,  
 Via Pietro Giuria 1, 10125 Torino, Italy.*

*Department of Physics, University of Durham,  
 South Road, Durham DH1 3LE, United Kingdom.*

**Abstract**

The complete matrix element for  $e^+e^- \rightarrow b\bar{b}Z^0 Z^0$  has been computed at tree-level and applied to  $Z^0 H^0$ -production followed by  $Z^0 \rightarrow b\bar{b}$  and  $H^0 \rightarrow Z^0 Z^0$ , including all the irreducible background, at Next Linear Colliders. We find that, assuming flavour identification of the  $Z^0$ -decay products, this channel, together with  $e^+e^- \rightarrow b\bar{b}W^+W^-$  in which  $Z^0 H^0 \rightarrow (b\bar{b})(W^+W^-)$ , can be important for the study of the parameters of the Standard Model Higgs boson over the heavy mass range  $2M_{Z^0} \lesssim M_{H^0} \lesssim 2m_t$ .

---

<sup>1</sup>Work supported in part by Ministero dell' Università e della Ricerca Scientifica.

## Introduction

Despite the innumerable phenomenological successes of the Standard Model ( $\mathcal{SM}$ ), an essential ingredient is still missing: the discovery of the Higgs boson  $H^0$ . This particle plays a crucial role in generating the spontaneous symmetry breaking of the  $SU(2)_L \times U(1)_Y$  gauge group of the electroweak interactions, and in ensuring the renormalizability of the whole theory. We know that the  $H^0$  is supposed to be a  $\mathcal{CP}$ -even neutral scalar boson, we know its couplings to the other elementary particles, but no prediction on its mass (i.e.,  $M_{H^0}$ ) can theoretically be done.

However, an upper bound of approximately 1 TeV (from perturbative unitarity arguments [1]) is expected, whereas a lower limit can be derived from current experiments at LEP I. In fact, from unsuccessful searches for  $e^+e^- \rightarrow Z^0 \rightarrow Z^{0*}H^0$  events at the  $Z^0$ -peak, one can deduce the bound  $M_{H^0} \gtrsim 60$  GeV [2].

Assuming the above mass range, various studies on the feasibility of its detection by the next generation of high energy machines have been carried out, both at hadron colliders [3, 4, 5, 6] and at the  $e^+e^-$  ones [3, 7, 8, 9, 10, 11].

On the basis of the expected center-of-mass (c.m.) energies, luminosities, detector performances of these accelerators and of the predicted cross sections and branching ratios, it has been definitively demonstrated that, if the  $H^0$  is in the mass region  $M_{H^0} \lesssim M_{Z^0}$  (i.e., light Higgs), it can be discovered at LEP II (with  $\sqrt{s_{ee}} = 160 \div 200$  GeV) in a large variety of channels [7]. For a larger mass Higgs, a  $pp$  colliders like the LHC ( $\sqrt{s_{pp}} = 14$  TeV) and/or an  $e^+e^-$  accelerator like the Next Linear Collider (NLC, with  $\sqrt{s_{ee}} = 300 \div 1000$  GeV) is needed. Even though at the LHC the mass range  $M_{Z^0} \lesssim M_{H^0} \lesssim 130$  GeV is quite difficult to cover since in this case the Higgs boson mainly decays to  $b\bar{b}$ -pairs (signature which has a huge QCD background if  $b$ -quarks cannot be recognized), nevertheless, it should be possible to detect it in the rare  $\gamma\gamma$ -decay mode [12] via the associated production with a  $W^\pm$  boson [13, 14] or a  $t\bar{t}$ -pair [15, 16]. At the LHC, for  $M_{H^0} \gtrsim 130$  GeV, the “gold-plated” four-lepton mode (i.e.,  $H^0 \rightarrow Z^0 Z^0 \rightarrow \ell^+ \ell^- \ell^+ \ell^-$ ), via various production channels, remains the clearest signature [4, 5]. At NLCs, with  $\sqrt{s_{ee}} = 300 \div 500$  GeV, the Higgs detection is possible over the whole intermediate mass range (i.e.,  $M_{Z^0} \lesssim M_{H^0} \lesssim 2M_{W^\pm}$ ) [17], via the bremsstrahlung reaction  $e^+e^- \rightarrow Z^{0*} \rightarrow Z^0 H^0$  [18] and/or the fusion processes  $e^+e^- \rightarrow \bar{\nu}_e \nu_e W^{\pm*} W^{\mp*} (e^+e^- Z^{0*} Z^{0*}) \rightarrow \bar{\nu}_e \nu_e (e^+e^-) H^0$  [19]. If  $\sqrt{s_{ee}} \gtrsim 500$  GeV, a heavy Higgs (i.e.,  $M_{H^0} \gtrsim 2M_{W^\pm}$ , and mainly produced via the fusion processes), can be detected via the four-jet modes  $H^0 \rightarrow W^\pm W^\mp, Z^0 Z^0 \rightarrow jjjj$  as well as via the  $4\ell$ -

decay [20, 21]. Finally, signatures that can be disentangled through  $b$ -tagging [22], must also be added to the mentioned channels: such as, e.g., at the LHC,  $t\bar{t}H^0$  production, with one  $t(\bar{t})$  decaying semileptonically and  $H^0 \rightarrow b\bar{b}$ , with  $80 \text{ GeV} \lesssim M_{H^0} \lesssim 130 \text{ GeV}$  [23].

In a recent study [24], we presented an analysis of the Bjorken reaction  $e^+e^- \rightarrow Z^0H^0$  in the case of a heavy Higgs decaying to  $W^+W^-$ -pairs and with  $Z^0 \rightarrow b\bar{b}$ , and of all the  $b\bar{b}W^+W^-$  irreducible background, assuming flavour identification of the  $Z^0$ -decay products. We emphasized in that work the importance of  $b$ -tagging the weak boson  $Z^0$ , as this could be one of the most efficient ways of detecting it, since this channel is free from  $W^\pm$ -decay backgrounds, has a branching ratio approximately five times larger than that one of  $Z^0$  decaying to  $\ell^+\ell^-$ -pairs (with  $\ell = e, \mu$  or  $\tau$ ), and is comparable to the fraction of invisible decays  $Z^0 \rightarrow \nu\bar{\nu}$ . This, obviously, relies on the expected efficiencies and purities for  $b$ -tagging at NLCs [25].

In ref. [24] we found that, after carrying a missing mass analysis [26] on  $e^+e^- \rightarrow b\bar{b}W^+W^-$ , there are values of the Higgs mass for which a simple cut on the invariant mass  $M_{b\bar{b}}$  is sufficient in order to completely eliminate the irreducible background (which is dominated by  $t\bar{t}$ -production and decay) when the double distributions  $d\sigma/dM_{b\bar{b}}/dM_{W^+W^-}$  of signal and background events do not overlap in the plane  $(M_{b\bar{b}}, M_{W^+W^-})$ . Otherwise, further cuts based on the kinematics of the  $t\bar{t}$ -background are needed, and these still maintain an acceptable number of events from Higgs production.

The missing mass method has the useful feature of being independent of assumptions on the  $H^0$ -decay modes, but this means that as the  $b\bar{b}W^+W^-$  events enter in the missing mass distribution so should the  $b\bar{b}Z^0Z^0$  ones, and with a quite large component of signal  $H^0 \rightarrow Z^0Z^0$  if compared to  $H^0 \rightarrow W^+W^-$ , since the  $Z^0Z^0$ -branching ratio is only a factor of two/three less than the  $W^+W^-$ -one in the heavy Higgs mass region (with  $M_{H^0} \lesssim 2m_t$ ). Because of this “inclusive” analysis on the decay products of the Higgs boson, both signals and irreducible backgrounds of both the above processes must be then considered at the same time<sup>2</sup>. Therefore, we retain that a complete study, which includes  $e^+e^- \rightarrow b\bar{b}Z^0Z^0$  as well as  $e^+e^- \rightarrow b\bar{b}W^+W^-$ , is needed in order to definitively establish the feasibility of all the foreseen measurements of the Higgs boson parameters, if the missing mass analysis is adopted and the  $Z^0$  is assumed to decay to  $b\bar{b}$ -pairs, with

---

<sup>2</sup>Moreover, in the range  $2M_{W^\pm} \lesssim M_{H^0} \lesssim 2m_t$ ,  $H^0 \rightarrow W^+W^-$  and  $H^0 \rightarrow Z^0Z^0$  are the only relevant branching fractions.

these tagged by vertex detectors.

As already done in ref. [24] we do not include in our computations the beam energy spread resulting from bremsstrahlung and beamsstrahlung effects, therefore, as explained there, one has to expect both the number of events and their statistical significance to be slightly higher than those ones we predict here.

In this letter, using the full matrix element for the process  $e^+e^- \rightarrow b\bar{b}Z^0Z^0$  we study the production of a heavy  $\mathcal{SM}$  Higgs (i.e.,  $M_{H^0} \geq 2M_{W^\pm}$ ) via the Bjorken bremsstrahlung reaction  $e^+e^- \rightarrow Z^0H^0$ , followed by the decays  $Z^0 \rightarrow b\bar{b}$  and  $H^0 \rightarrow Z^0Z^0$ , and of all the irreducible  $b\bar{b}Z^0Z^0$  background. Moreover, we present final results in which both the rates for  $b\bar{b}W^+W^-$  and  $b\bar{b}Z^0Z^0$  are added together.

Following the track of ref. [24], we give details of the calculation in section II, while in section III we present and discuss the results. Finally, section IV is devoted to our conclusions.

## Calculation

All the Feynman diagrams describing the process  $e^+e^- \rightarrow b\bar{b}Z^0Z^0$  at tree-level are shown in fig. 1, where graphs in which  $Z^0$ 's can be exchanged (i.e., when they do not come from the same vertex) must be counted twice (exchanging the corresponding quadrimomenta). The matrix element has been computed using the method of ref. [27] and we have checked the FORTRAN code for BRS invariance [28] and compared it with a second one, produced by MadGraph [29] and using the package HELAS [30]<sup>3</sup>.

The following numerical values of the parameters were adopted:  $M_{Z^0} = 91.1$  GeV,  $\Gamma_{Z^0} = 2.5$  GeV,  $\sin^2(\theta_W) = 0.23$ ,  $m_b = 5.0$  GeV and  $\alpha_{em} = 1/128$ . For the Higgs width (i.e.,  $\Gamma_{H^0}$ ) we have adopted the tree-level expression, and we have not included effects of the width of the final state  $Z^0$ 's.

A few thoughts will now be devoted to the procedure adopted for the integration of the matrix element over the phase space. In order to control the interplay between the various peaks which appear in the integration domain when all tree-level contributions are kept into account, we have split the Feynman amplitude squared into a sum of different (non gauge invariant) terms, each of which corresponds to the modulus squared of the resonant diagrams (for each possible resonance) and, eventually, their interference with other channels [24]. In a similar way, the contribution of non-resonant diagrams must also be considered.

---

<sup>3</sup>Running then only the first one for producing results.

Explicitly, in the case of the process  $e^+e^- \rightarrow b\bar{b}Z^0Z^0$  with  $M_{H^0} > 2M_{Z^0}$ , we have  $H^0 \rightarrow b\bar{b}Z^0$ ,  $Z^0 \rightarrow b\bar{b}$ ,  $H^0 \rightarrow Z^0Z^0$ ,  $Z^0H^0 \rightarrow (b\bar{b})(Z^0Z^0)$  and  $H^0 \rightarrow b\bar{b}$  resonances, via the five channels (see fig. 1)<sup>4</sup>:

$$\begin{aligned}
M_1 : & \quad H^0 \rightarrow b\bar{b}Z^0 && \text{diagrams \# 11, 12, 18,} \\
M_2 : & \quad Z^0 \rightarrow b\bar{b} && \text{diagrams \# 4, 5, 6 (with } Z^0 \text{ - propagators),} \\
M_3 : & \quad H^0 \rightarrow Z^0Z^0 && \text{diagrams \# 15, 16,} \\
M_4 : & \quad Z^0H^0 \rightarrow (b\bar{b})(Z^0Z^0) && \text{diagram \# 17,} \\
M_5 : & \quad H^0 \rightarrow b\bar{b} && \text{diagrams \# 13, 14.}
\end{aligned}$$

Diagrams # 1–3, 7–10, and 4–6 (with  $\gamma$  – propagators) constitute the sixth (non-resonant) channel ( $M_6$ ). Obviously, if  $M_i$  indicates the sum of the diagrams entering in the  $i$ -th channel, one has

$$M_{tot} = \sum_{i=1}^6 M_i, \quad (1)$$

where  $M_{tot}$  is the total Feynman amplitude. In squaring equation (1) we take the combinations<sup>5</sup>

$$\mathcal{M}_1^2 = |M_1|^2, \quad \mathcal{M}_2^2 = |M_2|^2 + 2\Re[M_2M_4^*], \quad (2)$$

$$\mathcal{M}_3^2 = |M_3|^2 + 2\Re[M_3M_4^*], \quad (3)$$

$$\mathcal{M}_4^2 = |M_4|^2, \quad \mathcal{M}_5^2 = |M_5|^2, \quad (4)$$

$$\begin{aligned}
\mathcal{M}_6^2 = & \quad |M_6|^2 \\
& + 2\Re[M_1M_2^*] + 2\Re[M_1M_3^*] + 2\Re[M_1M_4^*] + 2\Re[M_1M_5^*] \\
& + 2\Re[M_1M_6^*] + 2\Re[M_2M_3^*] + 2\Re[M_2M_5^*] + 2\Re[M_2M_6^*] \\
& + 2\Re[M_3M_5^*] + 2\Re[M_3M_6^*] + 2\Re[M_4M_5^*] + 2\Re[M_4M_6^*] \\
& + 2\Re[M_5M_6^*], \quad (5)
\end{aligned}$$

where  $\Re(x)$  represents the real part of  $x$ , and with

$$|M_{tot}|^2 = \sum_{i=1}^6 \mathcal{M}_i^2, \quad (6)$$

---

<sup>4</sup>Diagrams with exchanged  $Z^0$ 's are here implied.

<sup>5</sup>This in order to minimize the errors coming from the multi-dimensional integrations over the phase space, when we need to integrate interferences between channels with and without (or different) resonances.

where  $|M_{tot}|^2$  is the total Feynman amplitude squared.

Then, to obtain an integrand function smoothly dependent on the integration variables, for each contribution in the matrix element (6) containing a resonance we make the change

$$p^2 - M^2 = M\Gamma \tan \theta, \quad (7)$$

this factorizes the Jacobian

$$dp^2 = \frac{1}{M\Gamma} [(p^2 - M^2)^2 + M^2\Gamma^2] d\theta, \quad (8)$$

which removes the dependence on the Breit–Wigner peaks appearing in the  $\mathcal{M}_i^2$  terms. Here,  $p$ ,  $M$  and  $\Gamma$  stand for the quadrimomentum, the mass and the width of the resonance, respectively. Then, we separately integrated the various contributions (2)–(5) by VEGAS [31], using an appropriate phase space for each.

Finally, throughout this paper we adopt an integrated luminosity  $\mathcal{L} = 10 \text{ pb}^{-1}$  and we assume that only one  $b$ -jet is tagged, with an efficiency  $\epsilon_b = 1/3$  (i.e.,  $\epsilon_b$  is the probability for a  $b$ -quark to satisfy a given set of tagging requirements). Therefore, the probability of tagging at least one  $b(\bar{b})$  out of a  $b\bar{b}$ -pair is  $P_1 = 1 - (1 - \epsilon_b)^2 = 5/9 \approx 0.56$ . In principle, we should consider here the fact that there are also the other two  $Z^0$ 's in the event, one or both of which can decay to  $b\bar{b}$ -pairs. To this aim, we express  $P_n = 1 - (1 - \epsilon_b)^{2n}$  to be the probability of tagging at least one  $b(\bar{b})$  out of  $n$   $b\bar{b}$ -pairs, and we “roughly” split the total cross section  $\sigma(e^+e^- \rightarrow b\bar{b}Z^0Z^0)$  into three contributions:  $\sigma_3 = \sigma(e^+e^- \rightarrow b\bar{b}Z^0Z^0) \times [BR(Z^0 \rightarrow b\bar{b})]^2 \times \left(\frac{\delta_{b\bar{b},b\bar{b},b\bar{b}}}{\delta_{Z^0Z^0}}\right)$ ,  $\sigma_2 = \sigma(e^+e^- \rightarrow b\bar{b}Z^0Z^0) \times [2BR(Z^0 \rightarrow b\bar{b})] \times \left(\frac{\delta_{b\bar{b},b\bar{b}}}{\delta_{Z^0Z^0}}\right)$  and  $\sigma_1 = \sigma(e^+e^- \rightarrow b\bar{b}Z^0Z^0) - \sigma_2 - \sigma_3$ , corresponding to the case of three, two and one final  $b\bar{b}$ -pairs from  $Z^0$ -decays, respectively. Here,  $BR(Z^0 \rightarrow b\bar{b}) \approx 0.15$  is the  $Z^0$ -branching ratio into  $b$ -quarks, whereas  $\delta_{Z^0Z^0}(\delta_{b\bar{b},b\bar{b}})[\delta_{b\bar{b},b\bar{b},b\bar{b}}] = 1/2(1/4)[1/36]$  is the  $1/k!$  factor for each  $k$ -uple of identical particles (since we integrated over the whole phase space) in  $b\bar{b}XY(b\bar{b}b\bar{b}X)[b\bar{b}b\bar{b}b\bar{b}]$  final states, with  $X$  and  $Y$  not representing  $b$ -particles. Then, we expect the efficiency of tagging at least one  $b(\bar{b})$  out of all the possible final signatures of  $b\bar{b}Z^0Z^0$  events to be  $P_{tot} \approx \sum_{n=1}^3 P_n \sigma_n / \sigma(e^+e^- \rightarrow b\bar{b}Z^0Z^0) \approx 0.59$ . Since adopting one or the other of the two values  $P_1$  and  $P_{tot}$  would not change the conclusions (see later on), as a first approximation we forget the complications due to possible  $b\bar{b}$ -decays of the on-shell  $Z^0$ 's in  $b\bar{b}Z^0Z^0$  events, and we continue to treat these latter “inclusively”<sup>6</sup>.

---

<sup>6</sup>Also, throughout the analysis we implicitly assume that we are always considering the right “ $b\bar{b}$ ”-pair (i.e., the tagged  $b(\bar{b})$  with the un-tagged  $\bar{b}(b)$  coming from the same  $Z^0$ ), this is due to the

## Results

Our results are presented throughout figs. 2–7, and in tabs. I–IV.

In figs. 2–3 we show the differential distribution  $d\sigma/dM_{Z^0Z^0}$  for  $e^+e^- \rightarrow b\bar{b}Z^0Z^0$  events, obtained from the full matrix element (i.e., summed over all the six contributions  $\mathcal{M}_i^2$ ), for two different values of the c.m. energy of a NLC, and for the same choice of Higgs masses adopted in ref. [24] (see figs. 3–4 there)<sup>7</sup>. As in ref. [24], in order to disentangle the signal  $Z^0H^0 \rightarrow (b\bar{b})(Z^0Z^0)$  from the irreducible background we have imposed a cut around the  $Z^0$  mass, requiring that  $|M_{Z^0} - M_{b\bar{b}}| < 10$  GeV. Also, since we are looking for events that have to be tagged by microvertex detectors, we selected only configurations with  $|\cos\theta_{b\bar{b}}| < 0.8$  [25, 26].

Both in fig. 2 and in fig. 3 the  $H^0 \rightarrow Z^0Z^0$  peaks appear clearly visible over the flat structure of the irreducible background, which (looking at the integrals of the various components (2)–(5) of the matrix element) appears to be dominated by the  $H^0 \rightarrow b\bar{b}Z^0$  (i.e.,  $\mathcal{M}_1^2$ ) and the  $Z^0 \rightarrow b\bar{b}$  (i.e.,  $\mathcal{M}_2^2$ ) contributions, which, obviously, largely pass the cut in  $M_{b\bar{b}}$ . Moreover, the cross section corresponding to  $\mathcal{M}_1^2$  is roughly equal to twice the signal (i.e., the integral of  $\mathcal{M}_4^2$ ) since these two processes can be approximated in terms of a *production*  $\times$  *decay* reaction  $e^+e^- \rightarrow Z^0H^0 \rightarrow Z^0(Z^0Z^0) \times BR(Z^0 \rightarrow b\bar{b})$ , with the  $Z^0 \rightarrow b\bar{b}$  decay corresponding, in one case, to a  $Z^0$  directly coming from the two-body Bjorken process (diagram #17) and, in the other case (the contribution to this resonance coming from the  $H^0 \rightarrow b\bar{b}$  decay followed by a  $Z^0$ -bremsstrahlung off  $b$ -lines is in fact negligible), to a  $Z^0$  from the  $H^0 \rightarrow Z^0Z^0$  decay (diagrams #18), and with differences (only a few fractions of picobarns for the integrated “cross sections”) coming from the different kinematics of the decaying  $Z^0$ 's<sup>8</sup>. The factor of two comes from having two  $Z^0$ 's in the  $\mathcal{M}_1^2$  contribution that can both decay to a  $b\bar{b}$ -pair. In the case of  $\mathcal{M}_2^2$  we have three  $Z^0$ 's produced via bremsstrahlung off the  $e^+e^-$  fermion line, underlying cut in  $M_{b\bar{b}}$ , which drastically suppresses (because of the narrowness of the  $Z^0$ -resonance) any contribution coming from wrong  $b(\bar{b})$ -*jet* combinations, with the *jet* eventually coming from  $Z^0$ -decays (as done in ref. [24]).

<sup>7</sup>Only the value  $M_{H^0} = 170$  GeV, there considered at  $\sqrt{s} = 350$  GeV, has been dropped here, since this case would correspond to a below threshold decay  $H^0 \rightarrow Z^{0*}Z^{0*} \rightarrow f\bar{f}f'\bar{f}'$  (where  $f^{(\prime)}$  stands for a lepton  $\ell$  or  $\nu_\ell$ , with  $\ell = e, \mu, \tau$ , or a light quark  $q = u, d, s, c, b$ ), with a six particle signature  $(b\bar{b})(f\bar{f})(f'\bar{f}')$ , which deserves a more complicated treatment than of the one we are interested in performing here.

<sup>8</sup>In the following we will speak of a “prompt  $Z^0$ ” for the case  $\mathcal{M}_4^2$  and of a “ $H^0$ -decay  $Z^0$ ” for  $\mathcal{M}_1^2$ . Also we will write “bremsstrahlung  $Z^0$ ” when we will intend to indicate a  $Z^0$  produced via the diagrams entering in  $\mathcal{M}_2^2$ .

with one of them decaying to the  $b\bar{b}$ -pair<sup>9</sup>.

In tab. I we present the expected number of signal ( $S$ ) and background ( $B$ ) events together with the statistical significance  $S/\sqrt{B}$ , for  $\mathcal{L} = 10 \text{ fb}^{-1}$  and  $\epsilon_b = 1/3$ , in a window of 10 GeV around the adopted values of the Higgs mass  $M_{H^0}$ , at  $\sqrt{s} = 350$  and 500 GeV, after the cuts in  $M_{b\bar{b}}$  and  $\cos\theta_{b\bar{b}}$  discussed above. Looking at the ratio  $S/\sqrt{B}$  it would seem that, even though with a small number of events in some instances, the signal is detectable. However, we have to remember that the final goal is to look at the spectrum in missing mass and at the total number of events when the rates for both signal and background of both the processes  $e^+e^- \rightarrow b\bar{b}Z^0Z^0$  and  $e^+e^- \rightarrow b\bar{b}W^+W^-$  are added together in an inclusive analysis. For that, we have plotted in figs. 4–5 the differential distribution  $d\sigma/dM_{VV}$ , which is the sum of the corresponding histograms of the two above processes (when  $VV = Z^0Z^0$  and  $W^\pm W^\mp$ ), for the usual combination of Higgs masses and c.m. energies (i.e., we sum the distributions in fig. 3(4) of [24] and in fig. 2(3) of this study). Then we have again integrated these curves in a window of 10 GeV around  $M_{H^0}$ , obtaining the total number of signal and background events (now picked out of the inclusive missing mass spectrum) and the corresponding significances shown in tab. II<sup>10</sup>.

From figs. 4–5 and tab. II it is then clear that adding together the missing mass spectra of the two processes increases the total significances, to  $\approx 18(14)[20]\%$  for  $\sqrt{s} = 350$  GeV and  $M_{H^0} = 185(210)[240]$  GeV and to  $\approx 35(36)[43]\%$  for  $\sqrt{s} = 500$  GeV and  $M_{H^0} = 210(250)[300]$  GeV, with respect to those ones obtained for the process  $e^+e^- \rightarrow b\bar{b}W^+W^-$  only [24]. Now, with the values of tab. II the only signal that still appears quite difficult to disentangle from the irreducible background is  $M_{H^0} = 300$  GeV at  $\sqrt{s} = 500$  GeV, this is also due to the fact that for this value of  $M_{H^0}$  the Higgs width is sizably large ( $\Gamma_{H^0} \approx 8.5$  GeV) and comparable to the one of the window in  $M_{VV}$  we integrate over (whereas this does not happen for the other cases, since for them we always have  $\Gamma_{H^0} < 4.1$  GeV, the value of  $\Gamma_{H^0}$  for  $M_{H^0} = 250$  GeV).

Of course, at this point we could decide to integrate over a larger window, retaining

---

<sup>9</sup>We wonder if the case  $\mathcal{M}_1^2$  has to be really considered as a background, since it includes a Higgs produced via the Bjorken reaction, even though not peaking in the missing mass spectrum: in fact not all the particles entering in the missing mass come from the  $H^0$ . By the way, its spectrum in this variable is quite flat and completely useless in disentangle  $H^0$ -signals with respect the other backgrounds.

<sup>10</sup>Since in [24] only the significances for the cases  $\sqrt{s} = 500$  GeV and  $M_{H^0} = 250$  and 300 GeV were given for the value of  $top$  mass here adopted, we list now the remaining ones: they are 8.50(8.36)[6.20] for  $\sqrt{s} = 350$  GeV and  $M_{H^0} = 185(210)[240]$  GeV, and 17.57 for  $\sqrt{s} = 500$  GeV and  $M_{H^0} = 210$  GeV.



then more signal, but for  $\sqrt{s} = 500$  GeV and (let us say)  $|M_{VV} - 300 \text{ GeV}| \lesssim 10 \text{ GeV}$  we would include also the region (around  $M_{VV} \approx 310 \text{ GeV}$ ) where the background from  $e^+e^- \rightarrow b\bar{b}W^+W^-$  is maximum (compare with fig. 4 of [24]). Therefore, this is not the best way to proceed, and in fact in ref. [24] it has instead been decided to apply cuts based on the kinematics of  $t\bar{t}$ -production and decay: i.e., we required that one of the  $W^\pm$ 's (let us say  $W^+$ ) failed in reproducing the kinematics of the  $t\bar{t}$ -final state when coupled with either of the two  $b$ 's, namely that  $m_t - 10 \text{ GeV} > |M_{W+b(W+\bar{b})}| > m_t + 10 \text{ GeV}$  and  $E_{beam} - 10 \text{ GeV} > |E_{W^+} + E_{b(\bar{b})}| > E_{beam} + 10 \text{ GeV}$ . But, even though these selection criteria are quite convenient [24], they require the decay products of the  $W^\pm$  to be tagged: that is, a further experimental detection effort is needed compared to the missing mass analysis which only requires tagging the  $b\bar{b}$ -system.

The effect of another additional cut can then be exploited. If we look at the spectrum in energy  $E_{b\bar{b}}$  of the  $b\bar{b}$ -pair, this (due to the  $Z^0H^0$  two-body kinematics of the Bjorken production) is “practically” mono-energetic for a pair coming from a prompt  $Z^0$ , whereas it appears quite broad if the pair is produced by a  $H^0$ -decay or a bremsstrahlung  $Z^0$  (figs. 6–7)<sup>11</sup>. Therefore, retaining only events in an appropriate window around the maximum in  $E_{b\bar{b}}$  could further reduce the two  $Z^0$ -resonant backgrounds (and not those only) with respect to the signal. Some care has to be taken in exploiting this possibility. In fact, the above spectrum is really mono-energetic only apart from photon bremsstrahlungs off  $e^+e^-$ -lines<sup>12</sup>. When such photons (namely Initial State Radiation, ISR) are included in the computation, the energy flowing in the first  $Z^0$ -propagator of diagram 17 is not a constant any longer. Therefore, the prompt  $Z^0$  spectra would appear broader than those ones plotted here. Nevertheless, since the mean  $e^+e^-$  c.m. energy loss  $\delta_{\sqrt{s}}$  due to ISR is, e.g.,  $\approx 5\%$  at  $\sqrt{s} = 500 \text{ GeV}$  [32], one can choose a window wide enough ( $\approx \delta_{\sqrt{s}} \times \sqrt{s}$ ) to prevent complications due to such effects<sup>13</sup>. The effectiveness of this cut is clear from tab. III, which presents the percentage of configurations that give an energy of the  $b\bar{b}$ -pair in a window of 25 GeV

<sup>11</sup>Concerning the case of bremsstrahlung  $Z^0$ 's it has to be remembered (see eq. (2)) that  $\mathcal{M}_2^Z$  includes also the interference of  $Z^0 \rightarrow b\bar{b}$  with the signal  $Z^0H^0 \rightarrow (b\bar{b})(Z^0Z^0)$ , whose effects appear clearly visible in the “half” small peak below the signal one, and which, at the end, slightly enhance the contribution of this background.

<sup>12</sup>Even though photon emission can happen also off  $b\bar{b}$ -lines, however this latter can easily be included in the invariant mass reconstructing the  $Z^0$ -peak. So, we do not stress this case further, here.

<sup>13</sup>The inclusion of Linac energy spread and beamsstrahlung should not drastically change this strategy, at least for the “narrow” D–D and TESLA collider designs (see ref. [32]).

around the peak  $E_{bb}^{max}$  for the above three  $b\bar{b}Z^0Z^0$  sub-processes.

So, finally, requiring for the  $e^+e^- \rightarrow b\bar{b}VV$  events to have energy of the  $b\bar{b}$ -pair in the above window around the maxima (which are  $\approx 138(124)[105]$  GeV for  $\sqrt{s} = 350$  GeV and  $M_{H^0} = 185(210)[240]$  GeV, and  $\approx 214(196)[168]$  GeV for  $\sqrt{s} = 500$  GeV and  $M_{H^0} = 210(250)[300]$  GeV for both the cases<sup>14</sup>  $VV = Z^0Z^0, W^+W^-$ ) and calculating the corresponding percentage of events passing this cut (now for all the components of both the processes  $e^+e^- \rightarrow b\bar{b}W^+W^-$  and  $e^+e^- \rightarrow b\bar{b}Z^0Z^0$ ) leads to the final number of signal and background events, and their statistical significances, given in tab. IV. From which we deduce that an additional simple cut in  $E_{bb}$  increases the ratios  $S/\sqrt{B}$  up to values such that Higgs detection should now be feasible everywhere just by adopting a pure missing mass analysis (i.e., without resorting to any identification of the decay products of the vector bosons).

## Conclusions

In summary, in this letter we studied the production of a heavy Higgs (with  $2M_{W^\pm} < M_{H^0} < 2m_t$ , where  $m_t = 175$  GeV) and a  $Z^0$  through the Bjorken bremsstrahlung reaction  $e^+e^- \rightarrow Z^0H^0$  at NLC energies, assuming  $H^0 \rightarrow Z^0Z^0$  and  $Z^0 \rightarrow b\bar{b}$  and requiring a single  $b$ -tagging for the  $Z^0$ -detection. We have also studied all the irreducible background in  $e^+e^- \rightarrow b\bar{b}Z^0Z^0$  events. We found that Higgs signals, which would be clearly detectable for  $e^+e^- \rightarrow b\bar{b}Z^0Z^0$  on their own, still remain once we add (as needed for the missing mass analysis) this process to  $e^+e^- \rightarrow b\bar{b}W^+W^-$ , where  $Z^0H^0 \rightarrow (b\bar{b})(W^+W^-)$  and which includes among the irreducible background the huge  $t\bar{t} \rightarrow b\bar{b}W^+W^-$  production and decay. This was done only by imposing the following cuts on the  $b\bar{b}$ -system:  $|\cos\theta_{b\bar{b}}| < 0.8$ ,  $|M_{b\bar{b}} - M_{Z^0}| < 10$  GeV and  $|E_{b\bar{b}} - E_{b\bar{b}}^{max}| < 12.5$  GeV, where  $E_{b\bar{b}}^{max}$  is the maximum in the energy spectrum of the  $b\bar{b}$ -pair, which is practically mono-energetic for the  $b\bar{b}$ -pair coming from a  $Z^0$  produced in the two-body Bjorken reaction. In particular, this latter cut turns out to be extremely useful in rejecting the  $t\bar{t}$ -background in  $e^+e^- \rightarrow b\bar{b}W^+W^-$  events, thus avoiding further cuts based on the  $t\bar{t}$ -kinematics, which, although useful to the above aim, imply tagging the decay products of one of the two  $W^\pm$ 's. In fact, this latter procedure diminishes the attractiveness of the missing mass analysis (which only requires tagging the  $b\bar{b}$ -system),

---

<sup>14</sup>We do not reproduce here the figures for  $e^+e^- \rightarrow b\bar{b}W^+W^-$ , since they do not differ too much from figs. 6-7: there the signal (various backgrounds) is(are) as narrow (broad with respect to the signal) as that (those) one(s) of  $e^+e^- \rightarrow b\bar{b}Z^0Z^0$ .

and also introduces a reduction factor in the statistics due to the branching ratio of the decaying  $W^\pm$ -boson.

## Acknowledgements

We are grateful to Tim Stelzer and Bas Tausk for useful suggestions and constructive discussions, to Alessandro Ballestrero and Ezio Maina for focusing our attention on some important aspects of the phenomenological analysis here presented, and to Ghadir Abu Leil for a careful reading of the manuscript.

## References

- [1] M. Veltman, *Phys. Lett.* **B70** (1977) 253;  
B.W. Lee, C. Quigg and G.B. Thacker, *Phys. Rev. Lett.* **38** (1977) 883; *Phys. Rev.* **D16** (1977) 1519.
- [2] ALEPH Collaboration, *Phys. Rep.* **216** (1992) 253;  
DELPHI Collaboration, *Nucl. Phys.* **B373** (1992) 3;  
L3 Collaboration, *Phys. Lett.* **B303** (1993) 391;  
OPAL Collaboration, *Phys. Lett.* **B253** (1991) 511.
- [3] J.F. Gunion, H.E. Haber, G.L. Kane and S. Dawson, “*The Higgs Hunter Guide*”, Addison-Wesley, Reading MA, 1990.
- [4] Proceedings of the “*Large Hadron Collider Workshop*”, Aachen, 4-9 October 1990, eds. G. Jarlskog and D. Rein, Report CERN 90-10, ECFA 90-133, Geneva, 1990.
- [5] Proceedings of the “*Summer Study on High Energy Physics in the 1990s*”, ed. S. Jensen, Snowmass, Colorado, 1988;  
Proceedings of the “*1990 Summer Study on High Energy Physics: Research Directions for the Decade*”, ed. E.L. Berger, Snowmass, Colorado, 1990.
- [6] J.F. Gunion and T. Han, *preprint* UCD-94-10, April 1994.
- [7] Proc. of the ECFA workshop on LEP 200, A. Bohm and W. Hoogland eds., Aachen FRG, 29 Sept.-1 Oct. 1986, CERN 87-08.

- [8] Proceedings of the Workshop “*Physics and Experiments with Linear Colliders*”, Saariselkä, Finland, 9-14 September 1991, eds. R. Orawa, P. Eerola and M. Nordberg, World Scientific Publishing, Singapore, 1992.
- [9] Proc. of the Workshop “ *$e^+e^-$  Collisions at 500 GeV. The Physics Potential*”, Munich, Annecy, Hamburg, 3-4 February 1991, ed. P.M. Zerwas, DESY pub. 92-123A/B, August 1992.
- [10] Proc. of the ECFA workshop on “ *$e^+e^-$  Linear Colliders LC92*”, R. Settles ed., Garmisch Partenkirchen, 25 July-2 Aug. 1992, MPI-PhE/93-14, ECFA 93-154.
- [11] Proc. of the I Workshop on Japan Linear Collider (JLC), KEK 1989, KEK-Report 90-2;  
Proc. of the II Workshop on Japan Linear Collider (JLC), KEK 1990, KEK-Report 91-10.
- [12] C. Seez et al., in ref.[4].
- [13] S.L. Glashow, D.V. Nanopoulos and A. Yildiz, *Phys. Rev.* **D18** (1978) 1724.
- [14] R. Kleiss, Z. Kunszt and W.J. Stirling, *Phys. Lett.* **B253** (1991) 269;  
M.L. Mangano, SDC Collaboration note SSC-SDC-90-00113.
- [15] R. Raitio and W.W. Wada, *Phys. Rev.* **D19** (1979) 941;  
J.N. Ng and P. Zakarauskas, *Phys. Rev.* **D29** (1984) 876.
- [16] J.F. Gunion, *Phys. Lett.* **B261** (1991) 510;  
W.J. Marciano and F.E. Paige, *Phys. Rev. Lett.* **66** (1991) 2433;  
A. Ballestrero and E. Maina, *Phys. Lett.* **B268** (1992) 437;  
Z. Kunszt, Z. Trócsányi and W.J. Stirling, *Phys. Lett.* **B271** (1991) 247;  
D.J. Summers, *Phys. Lett.* **B277** (1992) 366.
- [17] V. Barger, K. Cheung, A. Djouadi, B.A. Kniehl and P.M. Zerwas, *Phys. Rev.* **D49** (1994) 79.
- [18] J.D. Bjorken, Proceedings of the “*Summer Institute on Particle Physics*”, SLAC Report 198 (1976);  
B.W. Lee, C. Quigg and H.B. Thacker, *Phys. Rev.* **D16** (1977) 1519;  
J. Ellis, M.K. Gaillard and D.V. Nanopoulos, *Nucl. Phys.* **B106** (1976) 292;  
B.L. Ioffe and V.A. Khoze, *Sov. J. Part. Nucl.* **9** (1978) 50.

- [19] D.R.T. Jones and S.T. Petkov, *Phys. Lett.* **B84** (1979) 440;  
R.N. Chan and S. Dawson, *Phys. Lett.* **B136** (1984) 196;  
K. Hikasa, *Phys. Lett.* **B164** (1985) 341;  
G. Altarelli, B. Mele and F. Pitolli, *Nucl. Phys.* **B287** (1987) 205;  
B. Kniehl, *preprint* DESY 91-128, 1991.
- [20] V. Barger, K. Cheung, B.A. Kniehl and R.J. Phillips, *Phys. Rev.* **D46** (1992) 3725.
- [21] K. Hagiwara, J. Kanzaki and H. Murayama, *Durham Univ. Report* No. DTP-91-18, 1991.
- [22] *Solenoidal Detector Collaboration Technical Design Report*, E.L. Berger *et al.*, *Report* SDC-92-201, SSCL-SR-1215, 1992.
- [23] J. Dai, J.F. Gunion and R. Vega, *Phys. Rev. Lett.* **71** (1993) 2699;  
J. Dai, J.F. Gunion and R. Vega, *Phys. Lett.* **B315** (1993) 355.
- [24] A. Ballestrero, E. Maina and S. Moretti, *Phys. Lett.* **B335** (1994) 460.
- [25] H. Borner and P. Grosse-Wiesmann, in ref. [9].
- [26] P. Grosse-Wiesmann, D. Haidt and H.J. Schreiber, in ref. [9].
- [27] K. Hagiwara and D. Zeppenfeld, *Nucl. Phys.* **B274** (1986) 1.
- [28] K. Fujikawa, B.W. Lee and A.I. Sanda, *Phys. Rev.* **D6** (1972) 2923;  
C. Becchi, A. Rouet and B. Stora, *Comm. Math. Phys.* **42** (1975) 127; *Ann. Phys.* **98** (1976) 287;  
B.W. Lee, C. Quigg and H.B. Thacker, *Phys. Rev* **D16** (1977) 1519;  
M.S. Chanowitz and M.K. Gaillard, *Nucl. Phys.* **B261** (1985) 379;  
G.J. Gounaris, R. Kögerler and H. Neufeld, *Phys. Rev.* **D34** (1986) 3257.
- [29] T. Stelzer and W.F. Long, *Comp. Phys. Comm.* **81** (1994) 357.
- [30] E. Murayama, I. Watanabe and K. Hagiwara, HELAS: HELicity Amplitude Sub-routines for Feynman Diagram Evaluations, *KEK Report* 91-11, January 1992.
- [31] G.P. Lepage, *Jour. Comp. Phys.* **27** (1978) 192.
- [32] T. Barklow, P. Chen and W. Kozanecki, in ref. [9].

## Table Captions

**table I** The expected number of  $e^+e^- \rightarrow b\bar{b}Z^0Z^0$  signal and background events in the window  $|M_{H^0} - M_{Z^0Z^0}| < 5$  GeV and their statistical significance at  $\sqrt{s} = 350$  GeV and  $\sqrt{s} = 500$  GeV for a selection of Higgs masses after the cuts:  $|M_{Z^0} - M_{b\bar{b}}| < 10$  GeV and  $|\cos\theta_{b\bar{b}}| < 0.8$ . We assume that only one  $b$ -jet is tagged with efficiency  $\epsilon_b = 1/3$ . The luminosity is taken to be  $\mathcal{L} = 10 \text{ fb}^{-1}$ .

**table II** The expected number of signal and background events for  $e^+e^- \rightarrow b\bar{b}Z^0Z^0$  and  $e^+e^- \rightarrow b\bar{b}W^+W^-$  processes, added together, in the window  $|M_{H^0} - M_{VV}| < 5$  GeV and their statistical significance at  $\sqrt{s} = 350$  GeV and  $\sqrt{s} = 500$  GeV for a selection of Higgs masses after the cuts:  $|M_{Z^0} - M_{b\bar{b}}| < 10$  GeV and  $|\cos\theta_{b\bar{b}}| < 0.8$ . We assume that only one  $b$ -jet is tagged with efficiency  $\epsilon_b = 1/3$ . The luminosity is taken to be  $\mathcal{L} = 10 \text{ fb}^{-1}$ . Numbers corresponding to the contribution of  $e^+e^- \rightarrow b\bar{b}W^+W^-$  events are taken from ref. [24] (assuming  $m_t = 175$  GeV).

**table III** Percentage of events with energy of the  $b\bar{b}$ -pair  $E_{b\bar{b}}$  in the window  $|E_{b\bar{b}}^{max} - E_{b\bar{b}}| < 12.5$  GeV for the cases of a prompt  $Z^0$ , a  $H^0$ -decay  $Z^0$  and a bremsstrahlung  $Z^0$  (see in the text) at  $\sqrt{s} = 350$  and  $\sqrt{s} = 500$  GeV for a selection of Higgs masses after the cuts:  $|M_{Z^0} - M_{b\bar{b}}| < 10$  GeV and  $|\cos\theta_{b\bar{b}}| < 0.8$ .

**table IV** The expected number of signal and background events for  $e^+e^- \rightarrow b\bar{b}Z^0Z^0$  and  $e^+e^- \rightarrow b\bar{b}W^+W^-$  processes, added together, in the window  $|M_{H^0} - M_{VV}| < 5$  GeV and their statistical significance at  $\sqrt{s} = 350$  GeV and  $\sqrt{s} = 500$  GeV for a selection of Higgs masses after the cuts:  $|M_{Z^0} - M_{b\bar{b}}| < 10$  GeV,  $|\cos\theta_{b\bar{b}}| < 0.8$  and  $|E_{b\bar{b}} - E_{b\bar{b}}^{max}| < 12.5$  GeV. We assume that only one  $b$ -jet is tagged with efficiency  $\epsilon_b = 1/3$ . The luminosity is taken to be  $\mathcal{L} = 10 \text{ fb}^{-1}$ . Numbers corresponding to the contribution of  $e^+e^- \rightarrow b\bar{b}W^+W^-$  events are computed from ref. [24] (assuming  $m_t = 175$  GeV).

## Figure Captions

**figure 1** Feynman diagrams contributing in the lowest order to  $e^+e^- \rightarrow b\bar{b}Z^0Z^0$  (those ones obtainable by exchanging the two  $Z^0$  bosons are not shown). Internal wavy lines represent a  $\gamma$  or a  $Z^0$ , as appropriate. Internal dashed lines represent a Higgs boson.

**figure 2** The differential distribution  $d\sigma/dM_{Z^0Z^0}$  for  $e^+e^- \rightarrow b\bar{b}Z^0Z^0$  (full matrix element with all Higgs contributions), at  $\sqrt{s} = 350$  GeV, for  $M_{H^0} = 185$  GeV (continuous line),  $M_{H^0} = 210$  GeV (dashed line) and  $M_{H^0} = 240$  GeV (dotted line), with the following cuts:  $|M_{Z^0} - M_{b\bar{b}}| < 10$  GeV and  $|\cos\theta_{b\bar{b}}| < 0.8$ .

**figure 3** The differential distribution  $d\sigma/dM_{Z^0Z^0}$  for  $e^+e^- \rightarrow b\bar{b}Z^0Z^0$  (full matrix element with all Higgs contributions), at  $\sqrt{s} = 500$  GeV, for  $M_{H^0} = 210$  GeV (continuous line),  $M_{H^0} = 250$  GeV (dashed line) and  $M_{H^0} = 300$  GeV (dotted line), with the following cuts:  $|M_{Z^0} - M_{b\bar{b}}| < 10$  GeV and  $|\cos\theta_{b\bar{b}}| < 0.8$ .

**figure 4** The differential distribution  $d\sigma/dM_{VV}$ , for  $e^+e^- \rightarrow b\bar{b}Z^0Z^0$  and  $e^+e^- \rightarrow b\bar{b}W^+W^-$  processes (full matrix elements with all Higgs contributions), added together, at  $\sqrt{s} = 350$  GeV, for  $M_{H^0} = 185$  GeV (continuous line),  $M_{H^0} = 210$  GeV (dashed line) and  $M_{H^0} = 240$  GeV (dotted line), with the following cuts:  $|M_{Z^0} - M_{b\bar{b}}| < 10$  GeV and  $|\cos\theta_{b\bar{b}}| < 0.8$ . Plots corresponding to the contribution of  $e^+e^- \rightarrow b\bar{b}W^+W^-$  events are taken from ref. [24] (assuming  $m_t = 175$  GeV).

**figure 5** The differential distribution  $d\sigma/dM_{VV}$ , for  $e^+e^- \rightarrow b\bar{b}Z^0Z^0$  and  $e^+e^- \rightarrow b\bar{b}W^+W^-$  processes (full matrix elements with all Higgs contributions), added together, at  $\sqrt{s} = 500$  GeV, for  $M_{H^0} = 210$  GeV (continuous line),  $M_{H^0} = 250$  GeV (dashed line) and  $M_{H^0} = 300$  GeV (dotted line), with the following cuts:  $|M_{Z^0} - M_{b\bar{b}}| < 10$  GeV and  $|\cos\theta_{b\bar{b}}| < 0.8$ . Plots corresponding to the contribution of  $e^+e^- \rightarrow b\bar{b}W^+W^-$  events are taken from ref. [24] (assuming  $m_t = 175$  GeV).

**figure 6** The differential distribution  $d\sigma/dE_{b\bar{b}}/\sigma$  for the signal  $e^+e^- \rightarrow Z^0H^0$  with the  $b\bar{b}$ -pair coming from the prompt  $Z^0$  (continuous line), from a  $H^0$ -decay  $Z^0$  (dashed line) and from a bremsstrahlung  $Z^0$  (dotted line), at  $\sqrt{s} = 350$  GeV, for  $M_{H^0} = 185, 210$  and  $240$  GeV, with the following cuts:  $|M_{Z^0} - M_{b\bar{b}}| < 10$  GeV and  $|\cos\theta_{b\bar{b}}| < 0.8$ .

**figure 7** The differential distribution  $d\sigma/dE_{b\bar{b}}/\sigma$  for the signal  $e^+e^- \rightarrow Z^0H^0$  with the  $b\bar{b}$ -pair coming from the prompt  $Z^0$  (continuous line), from a  $H^0$ -decay  $Z^0$  (dashed line) and from a bremsstrahlung  $Z^0$  (dotted line), at  $\sqrt{s} = 500$  GeV, for  $M_{H^0} = 210, 250$  and  $300$  GeV, with the following cuts:  $|M_{Z^0} - M_{b\bar{b}}| < 10$  GeV and  $|\cos \theta_{b\bar{b}}| < 0.8$ .



$M_{H^0}$ (GeV)	Signal	Background	$S/\sqrt{B}$
$\sqrt{s} = 350$ GeV			
185	7.45	0.18	17.63
210	9.00	3.64	4.72
240	4.44	1.13	4.17
$\sqrt{s} = 500$ GeV			
210	6.78	0.058	28.20
250	4.93	0.73	5.75
300	2.51	0.51	3.52
$\mathcal{L} = 10 \text{ fb}^{-1} \quad \epsilon_b = 1/3$			

Table I

$M_{H^0}$ (GeV)	Signals	Backgrounds	$S/\sqrt{B}$
$\sqrt{s} = 350$ GeV			
185	47.85	22.79	10.02
210	32.47	11.53	9.56
240	15.06	4.06	7.47
$\sqrt{s} = 500$ GeV			
210	24.48	1.07	23.65
250	16.56	9.01	5.52
300	8.17	17.92	1.93
$\mathcal{L} = 10 \text{ fb}^{-1} \quad \epsilon_b = 1/3$			

Table II

$M_{H^0}$ (GeV)	Prompt $Z^0$	$H^0$ -decay $Z^0$	Bremsstrahlung $Z^0$
$\sqrt{s} = 350$ GeV			
185	98%	0.63%	27%
210	99%	56%	70%
240	98%	36%	61%
$\sqrt{s} = 500$ GeV			
210	98%	0.36%	18%
250	96%	23%	23%
300	91%	23%	22%
$Z^0 \rightarrow b\bar{b}$			

Table III

$M_{H^0}$ (GeV)	Signals	Backgrounds	$S/\sqrt{B}$
$\sqrt{s} = 350$ GeV			
185	47.43	18.60	11.00
210	32.08	5.97	13.13
240	14.79	1.40	12.50
$\sqrt{s} = 500$ GeV			
210	23.91	0.14	62.84
250	15.87	1.54	12.79
300	7.42	5.09	3.29
$\mathcal{L} = 10 \text{ fb}^{-1} \quad \epsilon_b = 1/3$			

Table IV

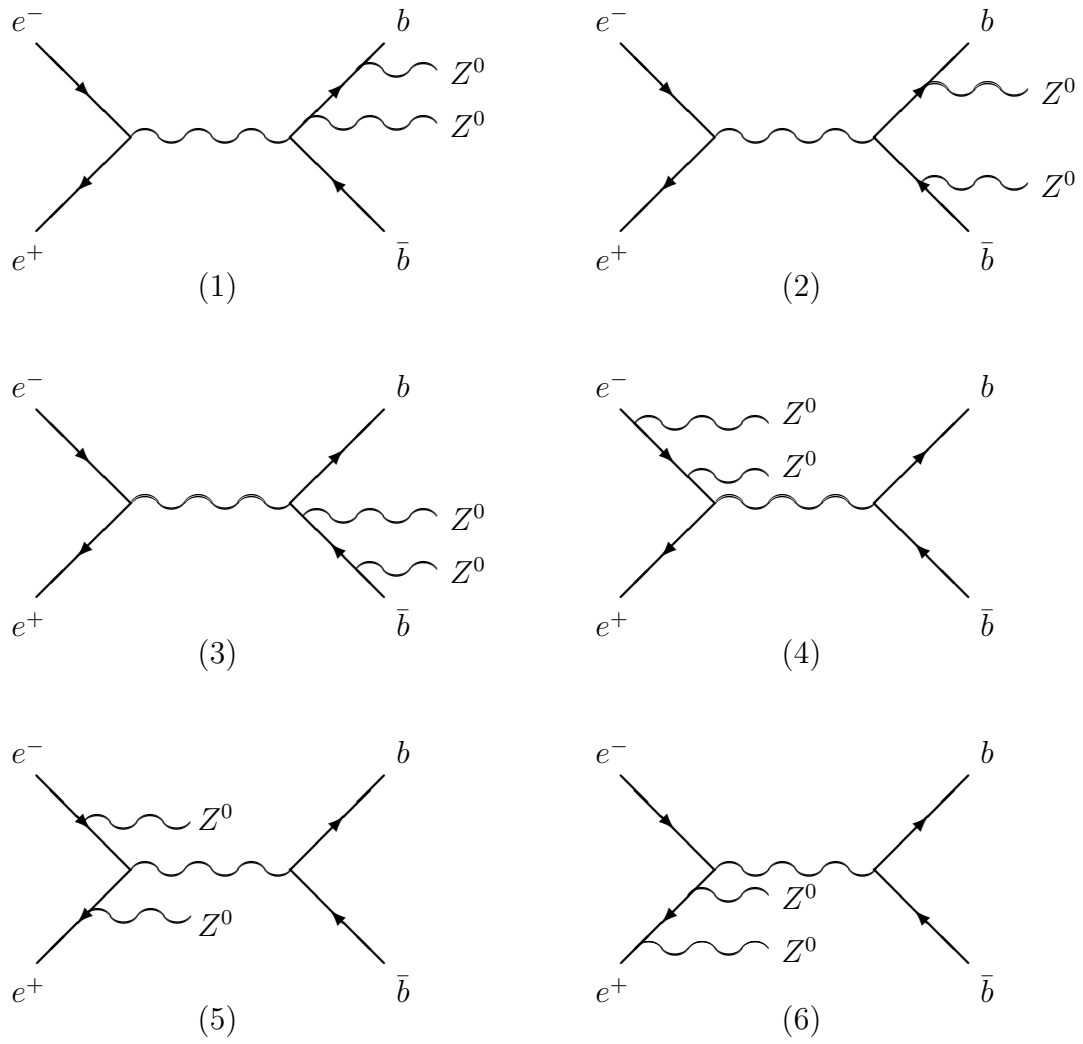


Figure 1

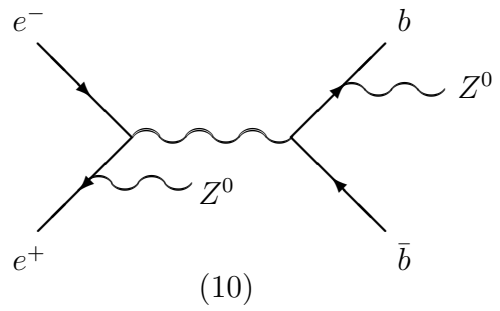
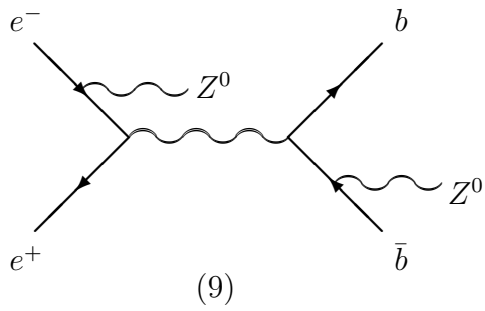
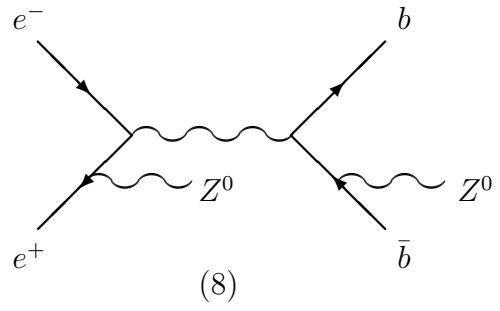
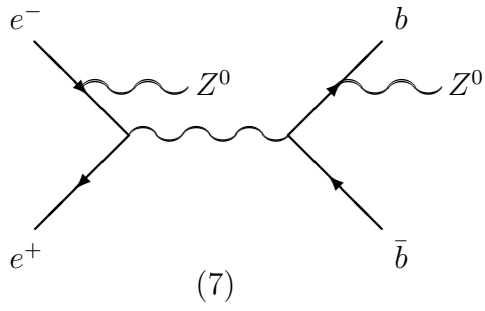


Figure 1 (Continued)

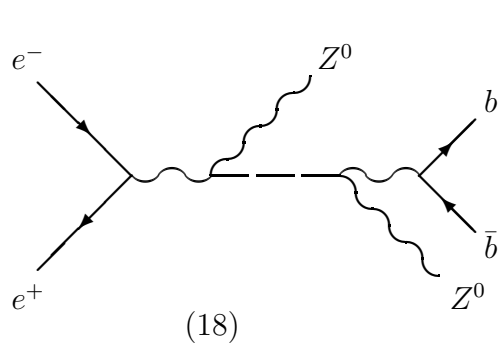
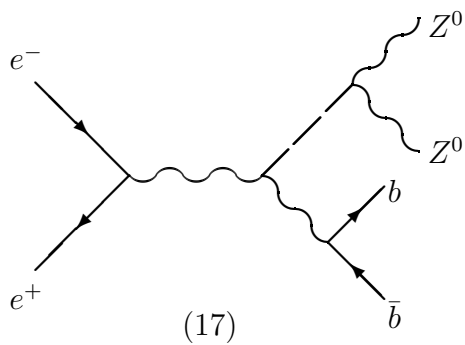
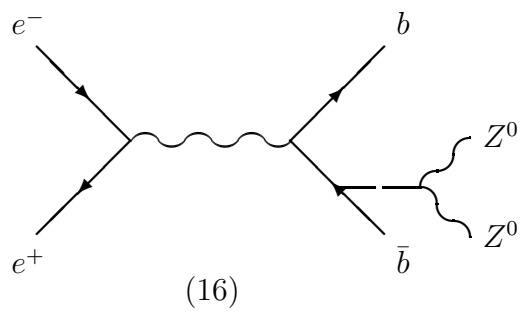
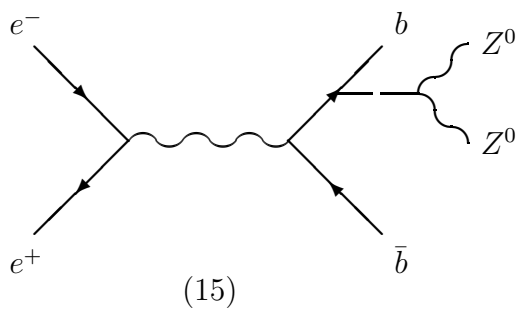
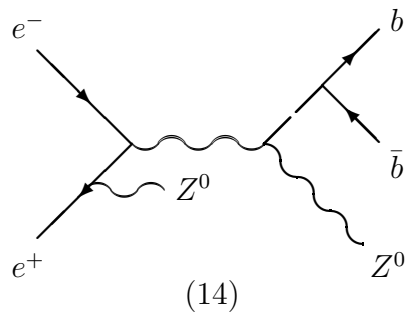
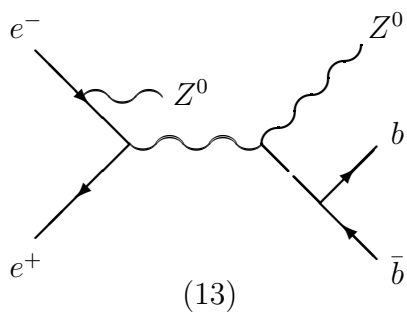
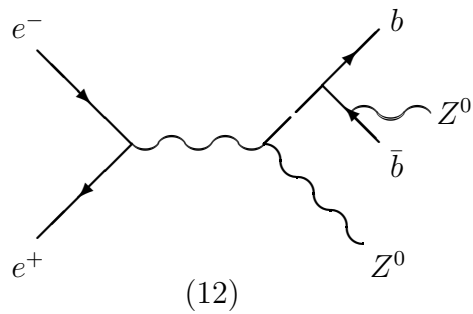
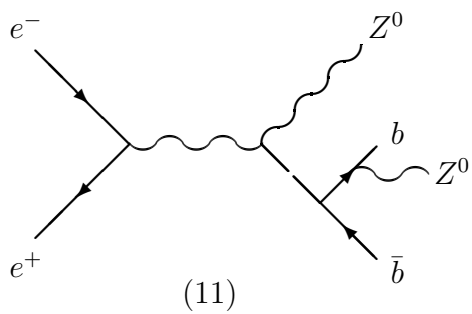


Figure 1 (Continued)

This figure "fig1-1.png" is available in "png" format from:

<http://arxiv.org/ps/hep-ph/9501300v1>



This figure "fig1-2.png" is available in "png" format from:

<http://arxiv.org/ps/hep-ph/9501300v1>

This figure "fig1-3.png" is available in "png" format from:

<http://arxiv.org/ps/hep-ph/9501300v1>

This figure "fig1-4.png" is available in "png" format from:

<http://arxiv.org/ps/hep-ph/9501300v1>

This figure "fig1-5.png" is available in "png" format from:

<http://arxiv.org/ps/hep-ph/9501300v1>

This figure "fig1-6.png" is available in "png" format from:

<http://arxiv.org/ps/hep-ph/9501300v1>